ACADEMIC PRESS

Available online at www.sciencedirect.com
SCIENCE DIRECT®

Journal of Catalysis 216 (2003) 213–222

JOURNAL OF CATALYSIS

www.elsevier.com/locate/jcat

Model catalysts: from imagining to imaging a working surface

D.W. Goodman

Department of Chemistry, Texas A&M University, PO Box 30012, College Station, TX 77842-3012, USA

Received 15 July 2002; revised 12 September 2002; accepted 21 October 2002

Abstract

Considerable progress has been made over the past two decades in spanning the well-known pressure and material gaps of heterogeneous catalysis. In particular, during the past decade several groups around the world have synthesized model catalysts consisting of metal clusters supported on planar oxide surfaces. These model catalysts are suitable for kinetic and spectroscopic investigations yet are amenable to study with scanning probe techniques at working temperatures and under realistic pressure conditions. This long-sought goal of observing a heterogeneous catalyst in an operating environment offers extraordinary new opportunities and poses significant new challenges for catalytic scientists of the 21st century. This article highlights some of these opportunities and challenges.

Keywords: Single crystals; Metal clusters; Quantum size effects; Thin film oxides

1. Introduction

Upon entering the basic catalysis arena more than two decades ago as a surface scientist, my goal and that of my colleagues was a rather simple one: to build a logical and seamless bridge between the traditional catalysis and surface science communities. Although considerable progress along these lines has been made, much remains to be done in achieving this unity and, more importantly, the common goal of our science, namely, an atomic-level understanding of heterogeneous catalytic processes. Ideally as fundamental catalytic scientists, we wish to relate microscopic properties such as atomic composition, electronic structure, and geometric structure to macroscopic properties such as catalytic activity and selectivity. Unfortunately, the complexity of "real world" catalysts often precludes a detailed knowledge of their microscopic properties. Fundamental studies using ultra high vacuum (UHV) methodologies offer an atomic-level view of a catalyst albeit the catalyst typically has been a single crystal surface at pressures on the order of 1×10^{-10} Torr. This UHV methodology obviously differs from that of real world catalysis with elevated pressures ($\geqslant 760$ Torr) and high-surface-area materials. In the past two decades remarkable strides have been made toward spanning these "material" and "pressure" divides, advances that permit studies of complex surfaces under realistic reaction conditions using a spectrum of surface science techniques.

The first divide to be spanned was the "pressure gap" that was addressed by combining UHV surface analytical techniques with an elevated pressure reactor system designed for measuring reaction kinetics [1–4]. These systems allow reaction kinetic measurements at elevated pressures without significantly disturbing the vacuum integrity of the primary UHV system. Measurements that combine surface science analytical techniques with reaction kinetics have been used to successfully span the so-called pressure gap for a variety of reactions.

The "materials gap" more recently has been spanned by the development of model catalysts that are similar to industrial catalysts in their complexity, but still suitable for modern surface analytical techniques [5–8]. These planar model catalysts consist of metal clusters deposited from either evaporative or molecular precursor sources onto metal oxide substrates. The use of thin oxide films circumvents the charging problems that make UHV studies of insulating supports such as SiO_2 or Al_2O_3 problematic [8].

In this article I would like to recount some of our success stories within the past two decades in our quest for a molecular-level view of catalysis and show how these studies have advanced our understanding of the working catalytic surface. New techniques such as polarization modulation infrared reflection absorption spectroscopy (PM-IRAS) now make it possible for us to "view" the working catalyst and

E-mail address: goodman@mail.chem.tamu.ed.

0021-9517/03/$ – see front matter
doi:10.1016/S0021-9517(02)00112-4

hold out the possibilities of "seeing" reaction intermediates in ways not possible two decades ago. In particular, the in situ capabilities of scanning probe microscopies are wonderfully suited for the task of "watching" the working catalyst and the morphological modifications that take place on a working catalyst. These stunning new experimental techniques combined with the powerful new theoretical methodologies promise to add new dimensions to our fundamental view of surface catalyzed reactions. This understanding will allow the next generation of catalytic scientists to begin their inquiries with a mental picture of a working catalyst that two decades ago would have been unimaginable. How we as chemists, physicists, and engineers utilize these insights to "design" the next generation of catalysts for the long-sought goals of complete selectivity with the utmost activity is to be seen. The magnitude and impact of the innovations to come will be limited only by the imagination and ingenuity of catalytic scientists.

2. The evolution of model catalysts

2.1. Metal single crystals

In the 1970s the simplest and thus most desirable model catalysts for combining kinetics under realistic conditions with surface analytical techniques were metal single crystals. These were first used in the pioneering studies of the Somorjai group [1]. At the National Bureau of Standards (now NIST) Dick Kelly, John Yates, Ted Madey, and I began studies in the mid-1970s of the methanation reaction over nickel single crystal surfaces [2]. These studies led to a careful comparison between the reaction kinetics measured under realistic conditions for single crystal catalysts and less ideal technical catalysts. The results of the two divergent catalysts proved to be amazingly similar and lent support for the use of single crystals as models for working catalysts, at least for certain reactions, i.e., structure insensitive reactions. In particular, methanation [2] and carbon monoxide oxidation [9], two well-known structure insensitive reactions, were extensively studied over a variety of single crystal catalysts and compared to the corresponding supported metal analogs. These comparisons were extremely favorable and demonstrated the insensitivity of these reactions to changes in the catalysts morphology and support. Later work in our laboratories addressed in great detail the influence of surface morphology on structure sensitive reactions, in particular the hydrogenolysis of alkanes [10]. Even for these reactions sensitive to surface structure, an interesting and surprising correspondence was observed between the single crystal catalysts and the corresponding supporting catalysts and showed the role of morphology in promoting C–C and C–H bond scission reactions. These studies led naturally to the study of the role of surface impurities in poisoning and promoting surface reactions and to the general observation that the surface modifier effect relates to the electronegative character of the impurity [11]. These single crystal studies in later years were extended to alloy surfaces and to the function and properties of mixed metals in altering catalytic activity and selectivity [12].

The requirement of UHV conditions for most surface analytical methods has limited the typical surface science inquiries to examination of the catalytic surface before and after reaction, or at minimum, to very restricted elevated pressure environments. More recently, however, the techniques of SFG [13,14] and PM-IRAS [15] have been used to investigate the surface of model catalysts under working conditions of temperature and pressure. For SFG, the laboratories of Somorjai/Shen [13] and Freund [14] have been active in applying this technique to in situ studies of catalytic surfaces. Our laboratories have recently used PM-IRAS to study the adsorption and reaction of CO and NO on a Pd(111) surface at pressures near 1 atm [16,17]. For CO on Pd(111), the coverage dependent overlayer structures were found to be identical over the pressure range from UHV to 800 mbar implying that no new surface species at elevated pressures or adsorbate-induced substrate reconstructions occur. For a reaction mixture of CO and NO at 240 mbar and 500–600 K, these studies show direct evidence for the formation of an isocyanate (–NCO) species as indicated in Fig. 1. In addition, below 0.01 mbar of CO and NO, no isocyanate features were detected illustrating the importance of carrying out in situ spectroscopic experiments under elevated pressure conditions with a surface specific technique such as PM-IRAS. Clearly the future will see more extensive use of these and other photon-in/photon-out techniques to probe catalytic surfaces with increasing complexity under realistic conditions.

These single crystal studies have demonstrated the relevance and utility of using simple single crystal surfaces to

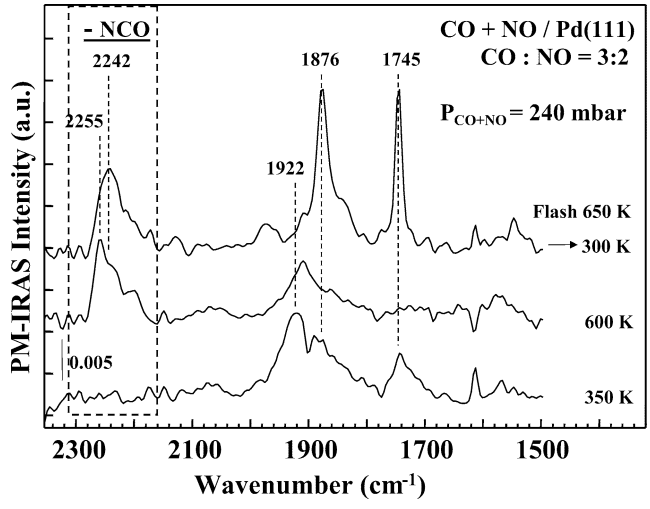

Fig. 1. In situ PM-IRA spectra of Pd(111) in the presence of a CO + NO mixture at 240 mbar (CO:NO = 3:2). The initial exposure was at $T_{surface} = 300$ K. At 600 K, i.e., under reaction conditions, the formation of an isocyanate-related feature at 2255 cm^{-1} is visible (highlighted in dashed-line box).

mimic more complex realistic catalyst systems. They also have highlighted in certain instances the need for a more complex model system to address the nuances of the actual working catalysts that are not accurately depicted with single crystals. This realization has led to the synthesis of supported metal clusters on planar oxide supports, an effort that has evolved considerably during the past ten years [18].

2.2. Planar oxide-supported metal clusters

2.2.1. Synthesis and characterization

The synthesis of a typical oxide-supported model catalyst is shown schematically in Fig. 2. The procedure is begun with a clean, refractory metal substrate, such as Mo, Ta, or Re. The structure of the substrate is chosen specifically to match the particular oxide film to be grown since crystal orientation and the nature of the interface are critical parameters in obtaining a high quality film. A thin metal oxide film, typically 1–10-nm thick, is then deposited onto the metal substrate by vapor deposition of the parent metal in an O_2 environment. Thin films of SiO_2 [19–21], Al_2O_3 [22–25], Ti_xO_y [26,27], MgO [28–31], NiO [32–35], and Fe_xO_y [36] have been prepared using this methodology. Finally, metal clusters are formed on the oxide thin film by vapor depositing the metal of choice. By the judicious control of the metal deposition parameters, metal clusters of varying size can be routinely achieved [37]. A variety of oxide/metal systems have been synthesized in our laboratories including Cu/SiO_2 [38,39], Pd/SiO_2 [40], Ni/SiO_2 [41], Pd/Al_2O_3 [42–44], Cu/Al_2O_3 [24,42], Au/Al_2O_3 [42], Ni/Al_2O_3 [45], Au/TiO_2 [46], and Pd/MgO [46]. Recently organometallic precursors have been used to prepare Ru/TiO_2 [47] and Au/TiO_2 [48] catalysts.

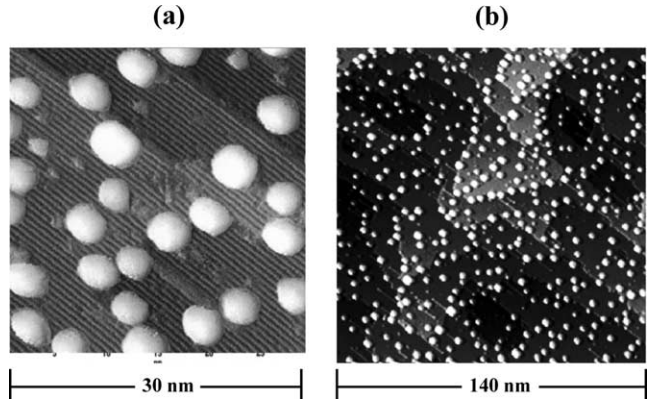

Fig. 3. (a) A constant current topographic–STM image of 0.25 mL Au deposited onto $TiO_2(110)$-(1×1). The sample was annealed to 850 K for 2 min; (b) general morphology of Au clusters on a $TiO_2(110)$ surface (2.0 V, 2.0 nA). The evaporation rate was 0.083 mL min^{-1} and the Au coverage was 1.0 mL.

Scanning tunneling microscopy (STM) is an indispensable technique for characterizing planar surfaces with sufficient conductivity. Fig. 3a shows a constant current topographic–STM micrograph of 0.25 mL Au deposited onto a single crystal $TiO_2(110)$ [49,50]. The deposition was performed at 300 K followed by an anneal of the TiO_2 surface to 850 K. Three-dimensional (3D) Au clusters have average diameters of ~ 2.6 and ~ 0.7 nm height (corresponding to 2–3 atoms thick) preferentially nucleate at step edges. Quasi-two-dimensional clusters are characterized by heights of 1–2 atomic layers [51]. An enlarged STM micrograph (140×140 nm^2) of a Au-covered (1.0 mL) $TiO_2(110)$ surface is shown in Fig. 3b. Hemispherical clusters with a narrow size distribution grow preferentially along the step edges with clusters on the flat terraces evident as well. At a Au coverage of 1.0 mL, more than 60% of the substrate is still

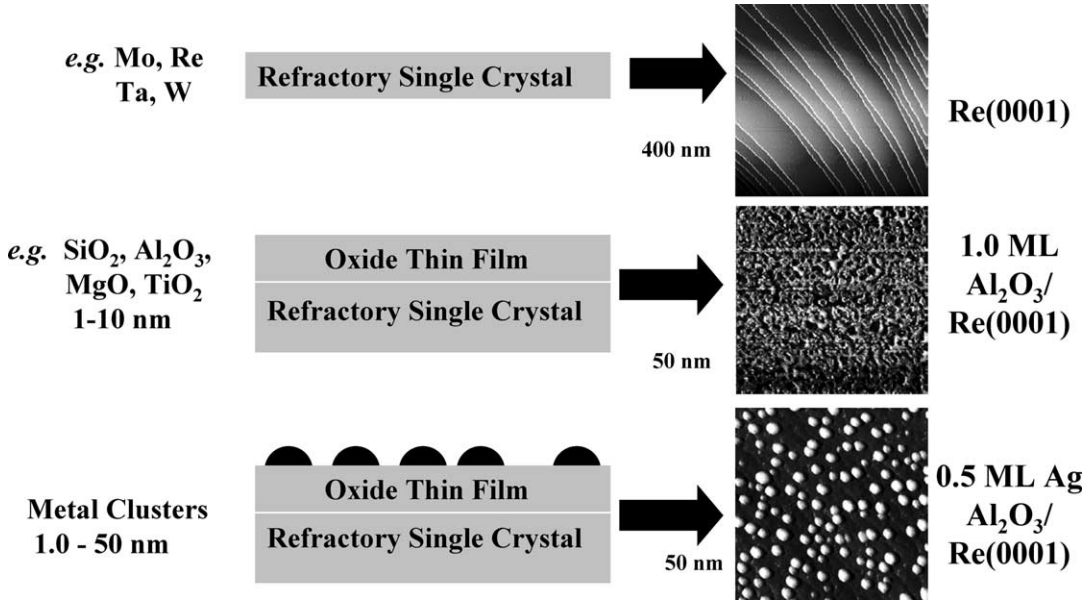

Fig. 2. Schematic of a planar oxide-supported model catalyst preparation procedure with the corresponding STM images of each stage.

metal-free and separated by monoatomic steps, consistent with 3D clustering or a Volmer–Weber growth mode.

The cluster size, in contrast to cluster density, increases continuously with metal coverage. For example, for Au/TiO_2, increasing the Au deposition from 0.10 to 2.0 mL increases the cluster size from 2.0 to 4.5 nm. This correlation between metal coverage and cluster diameter demonstrates that vacuum deposition can produce a specific size range and shape of metal clusters for model catalyst studies [52].

2.2.2. Reactivity studies: correlations from single crystals to technical catalysts

The CO methanation reaction ($CO + 3H_2 \rightarrow CH_4 + H_2O$) has been studied extensively over single crystal Ni(111) and Ni(100) catalysts [2,53], model $Ni/SiO_2/Mo(110)$ catalysts [41], and high surface area Ni/SiO_2 catalysts [54,55]. Fig. 4 compares the CO methanation rates (120 Torr total pressure and $H_2/CO = 4$) for a model Ni/SiO_2 catalyst and two different Ni/Al_2O_3 high-surface-area catalysts. The specific rates as well as the activation energies are in excellent agreement among the three catalysts. Kinetic studies for model Ni/SiO_2 catalysts with particle sizes ranging from 2 to 8 nm yielded specific reaction rates that were invariant with respect to particle size, consistent with the structure insensitivity of this reaction.

CO oxidation with O_2, a second well-known structure insensitive reaction, has been studied over Pd/SiO_2 model catalysts [56]. The reaction conditions were 10.0 Torr CO, 5.0 Torr O_2, and reaction temperatures in the range 540–625 K. Conversions were maintained at less than 50% and were measured by monitoring the pressure decrease in a static reactor of known volume. Fig. 5 shows Arrhenius plots of CO oxidation over three different model Pd/SiO_2 catalysts compared with a 5% loading of Pd on powder SiO_2 [56]. The average cluster sizes shown in Fig. 5 were determined by CO-temperature programmed desorption (TPD), O_2-TPD, and ex situ STM and atomic force microscopy. The specific reaction rates and activation energies for the model catalysts at somewhat higher temperatures compare favorably with the values extrapolated for the high-surface-area catalyst. There is no noticeable dependence of the CO_2 formation rate on the Pd cluster size, indicating that CO oxidation over Pd/SiO_2 is indeed structure insensitive.

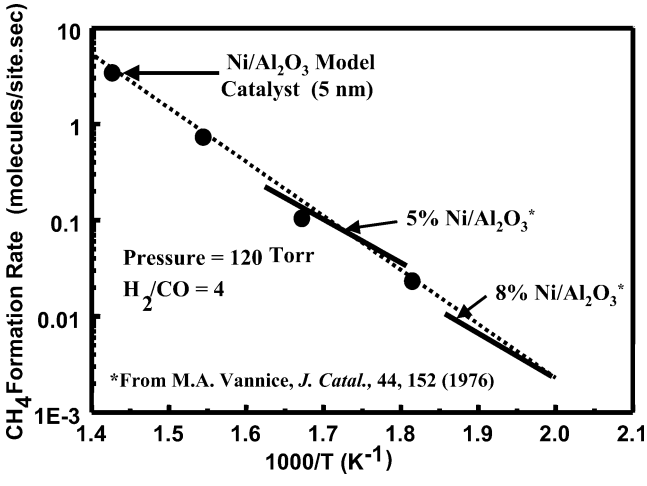

Fig. 4. CO methanation over model and conventional Ni/SiO_2 catalysts. Reaction conditions for the model studies were $P_{TOT} = 120$ Torr and $H_2/CO = 4$.

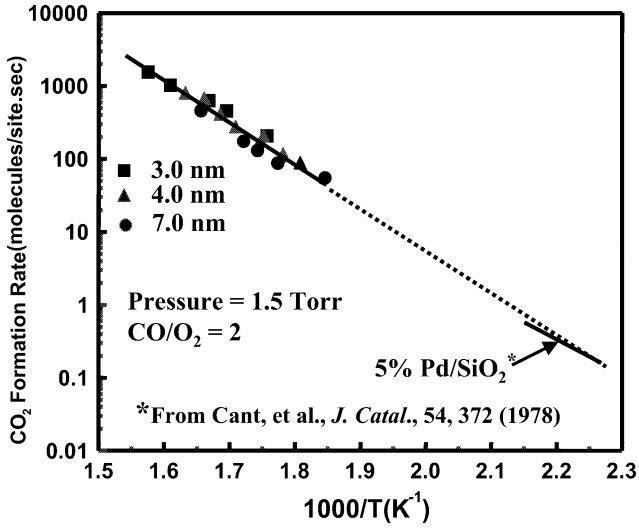

Fig. 5. CO oxidation with O_2 over model $Pd/SiO_2/Mo(100)$ and a conventional 5% Pd/SiO_2 catalyst. Reaction conditions for the model studies were $P_{TOT} = 1.5$ Torr and $CO/O_2 = 2$.

The oxidation of CO by NO was studied extensively over single crystal Pd(111) and Pd(100), model $Pd/Al_2O_3/Ta(110)$ catalysts, and conventional high surface area Pd/Al_2O_3 catalysts [44]. The single crystal and model supported catalyst data were acquired in a batch reactor at 2 Torr total pressure, with a $CO/NO \approx 1$. The data for the conventional supported catalysts were taken with a flow reactor at CO and NO partial pressures of 4.4 and 5.2 Torr, respectively. It is apparent from the data of Fig. 6 that the CO/NO reaction over Pd is structure sensitive. This conclusion is particularly obvious when the activity of the Pd/Al_2O_3 powder catalysts are compared—the most active catalyst has an average cluster size of 120 nm and an activity that is 30-fold higher than that catalyst with an average cluster size of 6 nm. Similar results were reported for the reaction of CO + NO over Rh clusters [57]. The single crystal results show that Pd(111) is five times more active than the more open (100) and (110) (not shown) surfaces [44,58,59]. It is also evident that the single crystals have higher activities and lower activation energies than the powder-supported catalysts, behavior similar to that reported for Rh catalysts [57,60].

IRAS results of CO adsorption experiments indicate that relatively large Pd clusters consist primarily of ⟨111⟩ and ⟨100⟩ facets [56], while Pd clusters less than 5.0 nm are characterized by less well-defined faceting and a large concentration of step edge/defect sites. With this consideration, the activities over supported clusters follow the same trend, as do the single crystal data; i.e., the smaller clusters behave like the more open single crystal surfaces and the large clusters, more like close-packed surfaces.

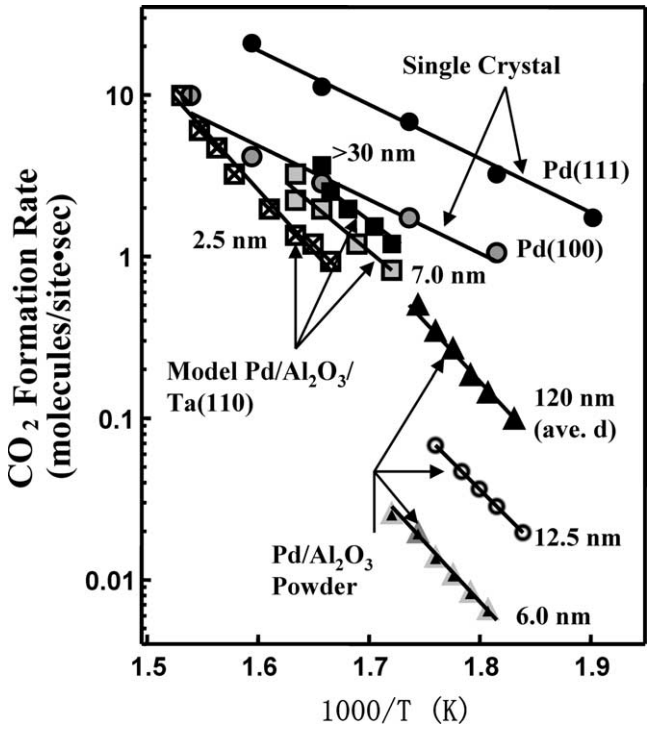

Fig. 6. CO + NO reaction over single crystal Pd, model $Pd/Al_2O_3/Ta(110)$ catalysts, and conventional high surface area Pd/Al_2O_3 catalysts. The powder catalysts were studied in a flow reactor ($P_{CO} = 4.4$ Torr and $P_{NO} = 5.2$ Torr). The single crystals and the model catalysts were studied in a batch reactor at 1 Torr partial pressure of CO and NO.

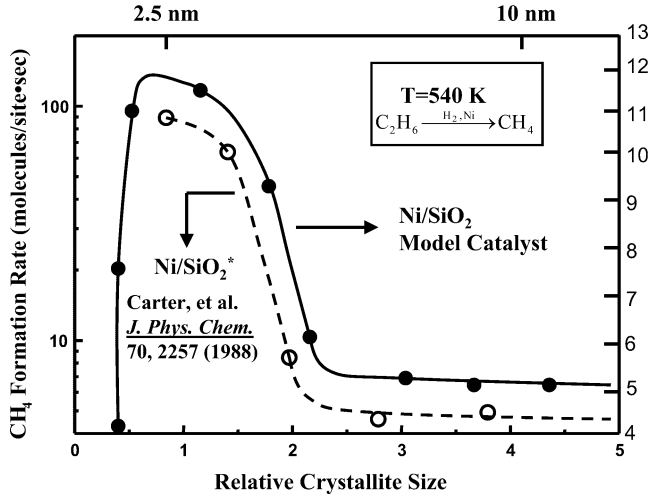

Fig. 7. CH_4 formation rate from ethane hydrogenolysis over model and conventional Ni/SiO_2 catalysts. For comparison data from Carter et al. [61] are included for supported Ni catalysts.

Studies of ethane hydrogenolysis over single crystal Ni(111) and Ni(100) surfaces have shown that the open (100) surface is significantly more active than the close-packed (111) surface [10]. In addition, the activation energy is substantially lower for the (100) face (100 kJ mol^{-1}) compared with the (111) face (192 kJ mol^{-1}). Earlier work on supported Ni catalysts has shown that a higher activity is observed for small metal particles compared with large metal particles [61]. Both electronic [62] and steric effects [63,64] have been proposed to explain the enhanced rates over Ni(100) surfaces. For example, the higher lying electronic levels of the Ni(100) surface compared with the Ni(111) surface could enhance the degree of backdonation into ethane antibonding orbitals thereby facilitating C–C bond scission. Alternatively, the more open Ni(100) surface could favor C–C bond scission and thus lower the activation barrier for this reaction compared with the (111) surface. Note that regardless of whether electronic or steric arguments are invoked, facile C–C bond breaking is the key to the enhanced activity of the (100) surface. This result implies that the rate determining step over the (100) surface is the hydrogenation of the stable carbidic or partially dehydrogenated carbonaceous species and that the rate determining step over the (111) surface is a C–C bond scission.

Studies over supported Ni catalysts have shown that there is an activity enhancement (on a per site basis) for smaller clusters relative to larger clusters, until a critical cluster size is reached, at which point the activity drops off rapidly [61, 64,65]. Fig. 7 compares the CH_4 formation rate at 540 K for model Ni/SiO_2 catalysts and traditional high surface area Ni/SiO_2 catalysts with varying particle sizes [54,55]. The structure sensitivity over both catalysts is evident. It is also apparent that the planar Ni/SiO_2 catalysts accurately model the high surface area supported Ni catalysts. Cluster size measurements of model Ni/SiO_2 catalysts indicate that the maximum in activity corresponds to a cluster size of ~ 2.5 nm. The single crystal kinetic results show that the size dependence of ethane hydrogenolysis over Ni clusters, at least to the optimum cluster size of ~ 2.5 nm, is related to the relative amounts of the (100) and (111) orientations on the surface of the clusters. There are several plausible explanations for the activity decrease below 2.5 nm. First, the Ni particles may exhibit an electronic modification from the bulk at or near 2.5 nm. Secondly, as the cluster size decreases, the interaction with the substrate may become more significant. Finally, the activity may relate to an ensemble effect, the requirement of multiple surface sites for reaction, that become limited as the particles become smaller. Whether one or more of these effects contribute significantly, recent work has shown that metal clusters of limited size, e.g., less than ~ 4 nm, have unique electronic and catalytic properties that are unlike the corresponding bulk metal. Perhaps the best studied system to date is nanosized gold clusters on certain oxide supports, e.g., TiO_2, with respect to the oxidation of carbon monoxide [49,66,67] and the selective oxidation of propylene [68].

2.2.3. The unique properties of nanocatalysts

Unique electronic and chemical properties are known to develop in solids when the dimensions of the solid reach the nanoscale [69–71]. These changes, which include discrete electronic structures, modified physical structures, and altered chemical reactivities, manifest themselves as new

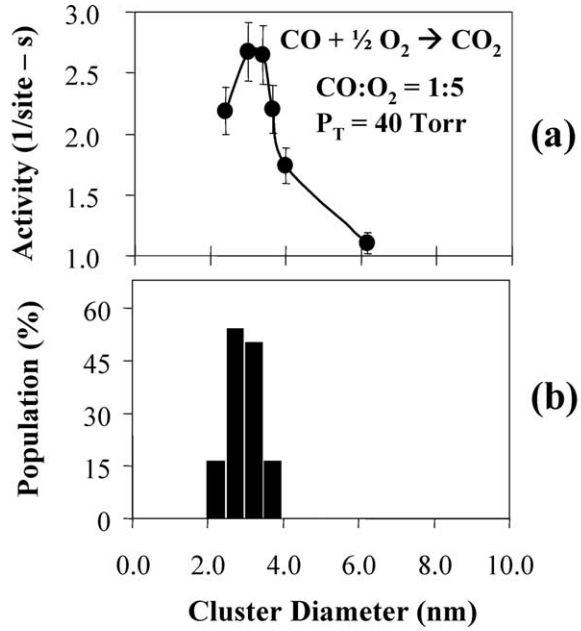

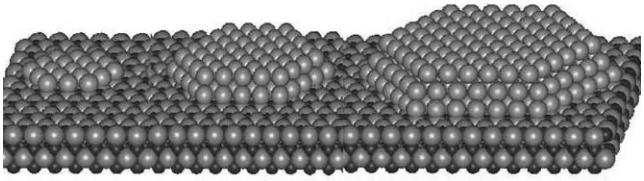

Fig. 8. (a) The activity for CO oxidation at 350 K as a function of Au cluster size supported on $TiO_2(110)$-(1×1) thin films grown on Mo(100). A 1:5 $CO:O_2$ mixture was used at a total pressure of 40 Torr. Activity is expressed as (product molecules) × (total Au atoms)$^{-1}$ s^{-1}; (b) a histogram of the distribution of cluster sizes. The schematic at the bottom shows the evolution of the cluster morphologies within the 0–10 nm range. The predominant morphology for the structures corresponding to those of the histogram is the indicated bilayer structure.

physical and chemical properties not observed in the "bulk" form of the material. Developing an understanding and ability to control the key features of nanoscale catalysts is a daunting scientific challenge, yet could lead to the long-sought goals of optimum catalytic activities combined with highly specific selectivities. Various explanations have been offered to account for the unique properties of nanoscaled metal catalysts [49,66,67], yet much remains to be understood.

A correlation has been observed between the Au cluster size and the catalytic activity for the partial oxidation of CO on $Au/TiO_2(110)$-(1×1). Fig. 8a shows a plot of the activity for CO oxidation (expressed as (product molecules) × (total Au atoms on surface sites)$^{-1}$ s^{-1} or turnover frequency (TOF)) at 350 K as a function of the size of Au clusters supported on a $TiO_2(110)$-(1×1) substrate [49,72]. The CO and O_2 (1:5 mixture of $CO:O_2$) reaction was carried out over Au/TiO_2 catalysts at 40 Torr total pressure [49,72]. A thin film of TiO_2 epitaxially grown on a Mo(100) substrate [26] onto which Au clusters were deposited was

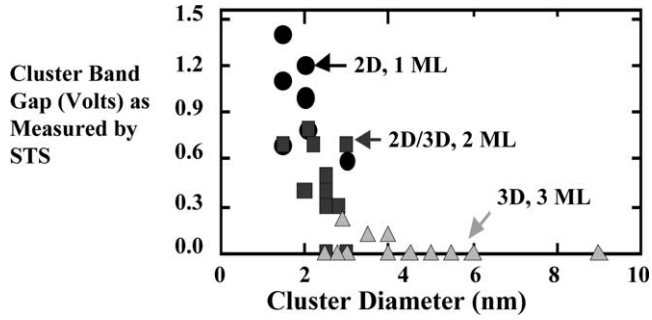

Fig. 9. Cluster band gaps measured by STS as a function of Au cluster size supported on $TiO_2(110)$-(1×1). The band gaps were obtained while the corresponding topographic scan was acquired on various Au coverages ranging from 0.2 to 4.0 mL. (●) Two-dimensional clusters; (■) 3D clusters, 2-atom layers in height; (▲) 3D clusters, 3-atom layers or greater in height.

used for the reaction kinetic measurements. STM images of Au deposited onto a $TiO_2(110)$-(1×1) single crystal were acquired in parallel with the kinetic measurements. The product (CO_2) was extracted from the reactor with a vacuum syringe, compressed, and analyzed with a GC. For each point in Fig. 8a a particular Au cluster size was prepared and then subjected to the $CO_2:O_2$ reaction. The cluster sizes of the Au particles and coverage of the surface sites obtained from parallel STM imaging experiments were used to calculate the TOF. The activity of the Au/TiO_2 catalysts exhibit a maximum TOF at an average Au cluster diameter of ~ 3.5 nm and decreases with an increase in diameter.

Fig. 8b is a histogram that shows the distribution of Au clusters with sizes ranging from 2.0 to 4.0 nm that are specifically two atoms thick (with diameters between 2.5 and 3.0 nm). The close correspondence between the maximum in the histogram and the maximum in the reactivity data suggests that two-atom-thick Au structures are optimally active for CO oxidation [49].

Fig. 9 shows a plot of the STS band gaps measured over the cluster size regime used for the $CO:O_2$ reactions of Fig. 8a. There is a correlation between the onset of catalytic activity and a metal-to-nonmetal transition in the supported Au clusters. The average Au cluster size where nonmetallic properties become apparent is 3.5 nm in diameter and 1.0 nm in height, corresponding to approximately 300 atoms per cluster. The square data in Fig. 9 are for those clusters two layers thick ranging in size from 2.0 to 4.0 nm in diameter and are those clusters which exhibit optimum catalytic activity for the CO oxidation reaction. The STS measured band gaps of this group of clusters range from 0.2 to 0.6 V. These results demonstrate that electronic properties as a function of cluster size play a crucial role in defining the catalytic reactivity of small metal clusters [49,72].

Thermodynamic data regarding the adsorption of CO on Au/TiO_2 catalysts with varying Au cluster sizes have been acquired with TPD using the well-known Redhead method [3] and with IRAS using the Clausius–Clapeyron relationship [73,74]. Results for the latter measurements are displayed in Fig. 10. CO adsorption on Au clusters larger

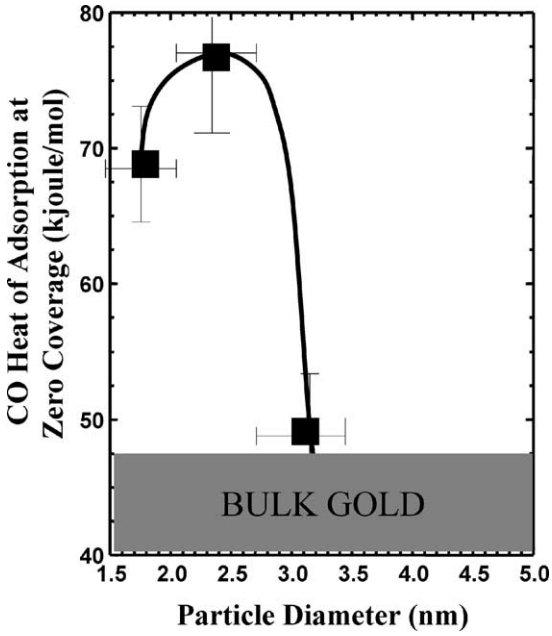

Fig. 10. CO heats of adsorption determined by the Clausius–Clapeyron method at a CO coverage of $< 10\%$ of saturation as a function of Au cluster size on a $TiO_2(110)$ support.

than ~ 4.0 nm behave as bulk Au. However, as the clusters become smaller the heat of CO adsorption increases from 12 kcal/mol to a maximum of 19 kcal/mol for clusters ~ 3.0 nm in diameter [4]. The data of Fig. 10 show a significant increase in the adsorption energy with a decrease in cluster size, with a maximum that correlates remarkably close to the maximum observed in the reactivity measurements of Fig. 8a. A similar increase in the binding energy of O_2 with a decrease in the Au cluster size on TiO_2 has been observed recently [75]. In any case, clearly the effects of cluster size on the adsorption properties of Au clusters is significant and likely a key to the altered catalytic properties displayed by ultra small Au clusters. Recent core level binding energies for the Au $4f_{7/2}$ core level as a function of Au cluster size on $TiO_2(110)$ and SiO_2 surfaces have been measured [50] and the differences shown to be a result of the relative strengths of the interaction of Au with these two different metal oxide supports. Related theoretical calculations [76] are consistent with this interpretation. For Au on TiO_2, the Au d bands are much closer to E_f due to charge polarization in the interfacial region and a subsequent increase of the potential in the adlayer. Such a large energy shift of the Au $5d$ band toward E_f should strongly alter the surface chemical properties of Au/TiO_2 from those of bulk Au [7].

Temperature programmed desorption is a useful tool for obtaining detailed information on adsorbate–surface bonding, adsorbate–adsorbate interactions, and desorption kinetics, and determining binding energies of metals adsorbed onto surfaces. TPD binding energy determinations also allow for comparative estimations of admetal cluster size on different oxide supports. In a series of TPD spectra acquired for Au on SiO_2, a marked decrease in the Au cluster binding energies, denoted by the peak temperature maximum (T_m) in the TPD of the clusters, is observed [50]. Fig. 11a shows a family of TPD spectra taken of the Au clusters deposited onto a SiO_2 thin film. The leading edge of the TPD peak maxima shifts to higher temperatures as the Au coverage increases. The inset shows a plot of the sublimation energy (E_{sub}) as a function of Au coverage, determined using the leading edge analysis [77]. At 0.2 mL, the E_{sub} at ~ 50 kcal mol^{-1} increases rapidly (with increasing Au coverage) to the bulk value at ~ 90 kcal mol^{-1} at 5.0 mL. The decrease in E_{sub} can be explained by the fact that an atom at the edge of a small cluster has fewer nearest neighbors than

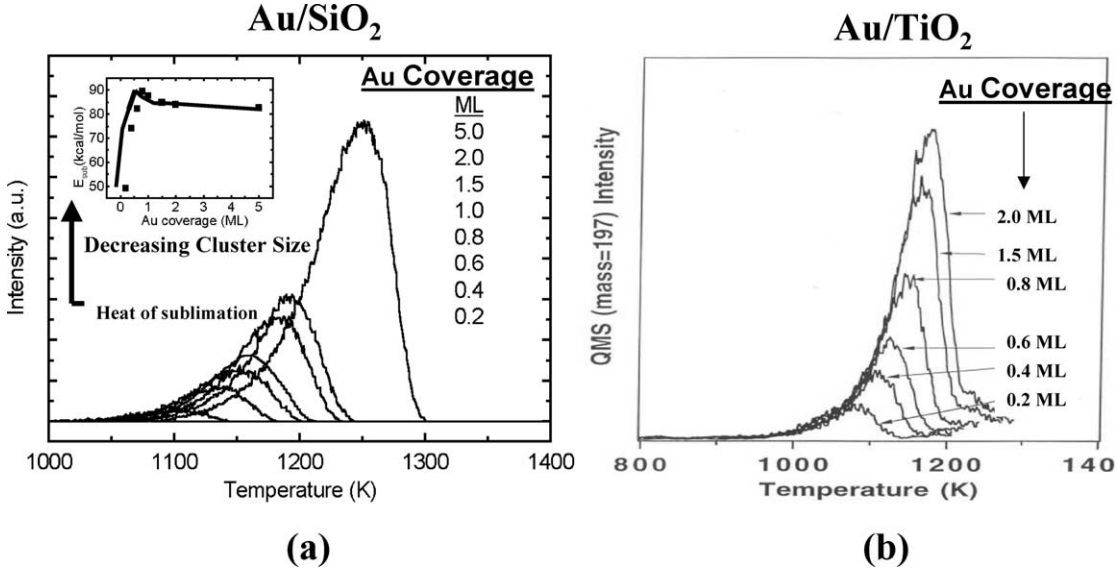

Fig. 11. A set of TPD spectra of Au ($m/e = 197$) from (a) a ~ 2.5 nm-thick SiO_2 thin film on Mo(110) and (b) a TiO_2 thin film on Mo(100) at Au coverages ranging from 0.2 to 5.0 mL. The inset in (a) shows a plot of E_{sub} determined via leading edge analysis.

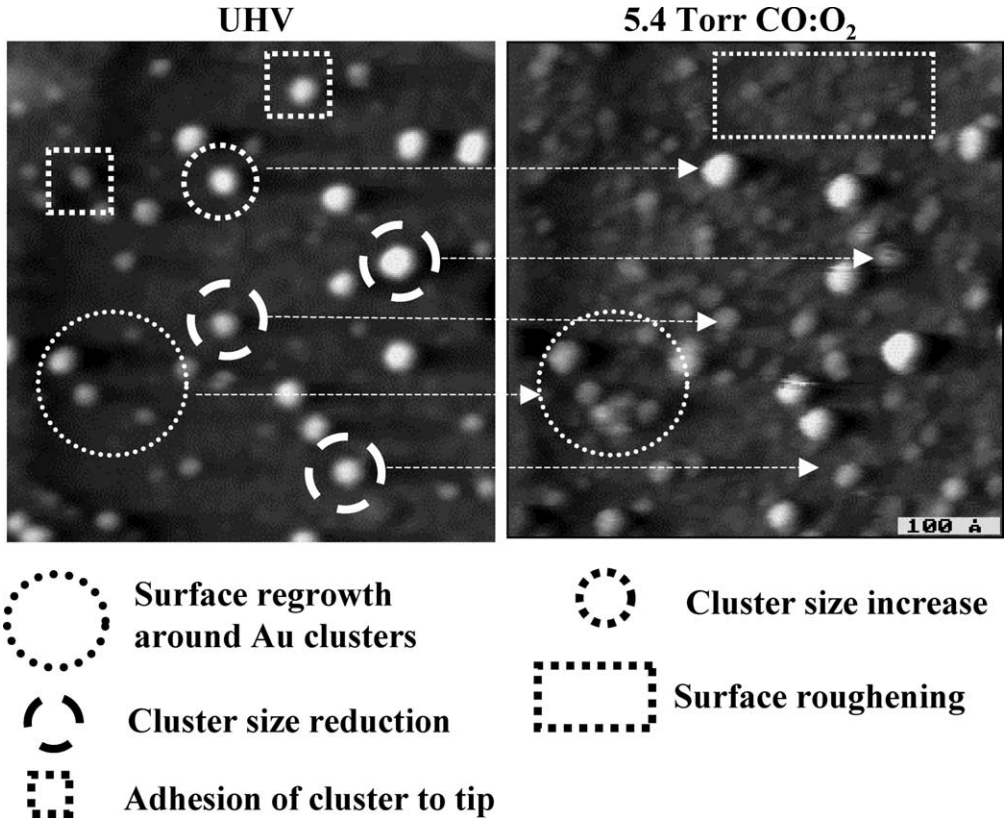

Fig. 12. A 50×50 nm^2 image of the same area acquired at 450 K: (left) under ultra high vacuum conditions and (right) during exposure to a reaction mixture consisting of a 665 Pa CO:O_2 mixture.

those in larger clusters and hence desorbs more easily due to decreased surface tension.

The interaction of Au with TiO_2(001) has also been determined using the same approach; the results are shown in Fig. 11b. In this case, however, only a single desorption feature is observed with a common leading edge for all Au coverages. With leading edge analysis, the Au binding energy on TiO_2(001) is estimated to be 50 kcal mol^{-1}, considerably smaller than the Au bulk sublimation energy of 90 kcal mol^{-1}. This dramatic decrease of the sublimation energies *at all cluster sizes*, from the smallest to the largest, is likely related to the relatively strong interaction between Au and the TiO_2 support. This strong interaction leads to a greater degree of wetting of TiO_2 by Au compared with Au/SiO_2, and therefore to greater dispersion of the Au on TiO_2. The lower sublimation energies found for the Au clusters on TiO_2 may arise due to the preferential evaporation of Au at the periphery of pseudo-planar Au clusters with relatively low-coordinated Au. In any case, this contrast of behavior regarding the sublimation of Au from SiO_2 and TiO_2 highlights the role of the support in altering the properties of ultra small clusters of Au.

The presence of reactant gases under realistic conditions can affect the admetal's ability to wet the surface and thereby alter particle size and distribution. For example, even though the TiO_2-supported Au catalysts exhibit a high activity for the low-temperature CO oxidation, the catalysts are often rapidly deactivated [72]; i.e., the CO conversion for a Au/TiO_2 catalyst is markedly attenuated as a function of reaction time. The deactivation is due to agglomeration of the Au clusters induced by interaction of O_2 with the Au clusters [78,79]. Recently a STM especially designed for in situ studies has been used in our laboratories to follow this deactivation [80]. In Fig. 12 a selected area is shown in (left) for UHV conditions and in (right) for 665 Pa of a CO:O_2 (1:5) reaction mixture over a Au/TiO_2 catalyst [79]. There are noteworthy parallels between the instability of the small Au clusters, their catalytic activity, and the change in their catalytic activity with time. Au clusters of approximately 3 nm are optimum as CO oxidation catalysts. It is apparent that reaction-induced sintering of these small clusters is a mechanism for the loss of activity with time. These preliminary investigations show the power of scanning probe microscopies to monitor changes in catalyst morphology *under realistic reaction conditions.* This capability does indeed alter the prospects of merely imagining the nature of the working surface to being able to image this surface with atomic resolution. This capability coupled with the use of in situ spectroscopies offers exciting prospects for detailing the morphology of the catalyst and speciation at its surface, all under realistic working conditions.

3. Conclusions and future prospects

The evolution of catalytic science during the past two decades has given us the capability of imaging the working surface while carrying out spectroscopies of surface species under realistic reaction conditions of pressure and temperature. Furthermore, advances in the synthesis of more complex model catalysts that more accurately reflect the nuances of the corresponding technical analogs have remedied to a large degree the material discrepancies evident in earlier surface science investigations. Advances in electron microscopy, free electron lasers, high brilliance photon-based microscopies, highly localized spectroscopies, etc., ultimately will allow the study of catalytic systems on a particle-by-particle basis, i.e., the acquisition of highly accurate structural data coupled with detailed surface speciation *on a specific cluster.* These capabilities coupled with improved synthetic routes to highly specific cluster sizes and morphologies will add new dimensions to our understanding of structure–function relationships in heterogeneous catalysis. Indeed, the next 40 years will most certainly be as exciting or more so than the past 40 years.

Acknowledgments

We acknowledge with pleasure the support of this work by the Department of Energy, Office of Basic Energy Sciences, Division of Chemical Sciences, and the Robert A. Welch Foundation.

References

[1] S.H. Kahn, G.A. Somorjai, J. Catal. 34 (1974) 294.
[2] D.W. Goodman, R.D. Kelley, T.E. Madey, J.T. Yates, J. Catal. 63 (1980) 226.
[3] H.P. Bonzel, H.J. Krebs, Surf. Sci. 91 (1980) 499.
[4] C.T. Campbell, M.T. Paffett, Surf. Sci. 139 (1984) 396.
[5] H.J. Freund, Surf. Sci. 500 (2002) 271.
[6] C.R. Henry, Surf. Sci. Rep. 31 (1998) 235.
[7] C.T. Campbell, Surf. Sci. Rep. 27 (1997) 1.
[8] D.W. Goodman, Surface Rev. Lett. 2 (1995) 9.
[9] P.J. Berlowitz, C.H.F. Peden, D.W. Goodman, J. Phys. Chem. 92 (1988) 5213.
[10] D.W. Goodman, Surf. Sci. 123 (1982) L679.
[11] D.W. Goodman, Acc. Chem. Res. 17 (1984) 194.
[12] J.A. Rodriguez, D.W. Goodman, Science 257 (1992) 897.
[13] G.A. Somorjai, Appl. Surf. Sci. 121 (1997) 1.
[14] T. Dellwig, G. Rupprechter, H. Unterhalt, H.J. Freund, Phys. Rev. Lett. 85 (2000) 776.
[15] G.A. Beitel, A. Laskov, H. Oosterbeek, E.W. Kuipers, J. Phys. Chem. 100 (1996) 12494.
[16] E. Osenzoy, D. Meier, D.W. Goodman, J. Phys. Chem. 106 (2002) 9376.
[17] C. Hess, E. Osenzoy, D.W. Goodman, J. Am. Chem. Soc. 124 (2002) 8524.
[18] P.L.J. Gunter, J.W. Niemantsverdriet, F.H. Ribeiro, G.A. Somorjai, Catal. Rev. Sci. Eng. 39 (1997) 77.
[19] J.W. He, X. Xu, J.S. Corneille, D.W. Goodman, Surf. Sci. 279 (1992) 119.
[20] X.P. Xu, D.W. Goodman, Appl. Phys. Lett. 61 (1992) 774.
[21] X.P. Xu, D.W. Goodman, Surf. Sci. 282 (1993) 323.
[22] P.J. Chen, D.W. Goodman, Surf. Sci. 312 (1994) L767.
[23] D.W. Goodman, J. Vac. Sci. Technol. A 14 (1996) 1526.
[24] M.C. Wu, D.W. Goodman, J. Phys. Chem. 98 (1994) 9874.
[25] X. Lai, C.C. Chusuei, K. Luo, Q. Guo, D.W. Goodman, Chem. Phys. Lett. 330 (2000) 226.
[26] W.S. Oh, C. Xu, D.Y. Kim, D.W. Goodman, J. Vac. Sci. Technol. A 15 (1997) 1710.
[27] Q. Guo, W.S. Oh, D.W. Goodman, Surf. Sci. 437 (1999) 49.
[28] J.S. Corneille, J.W. He, D.W. Goodman, Surf. Sci. 306 (1994) 269.
[29] M.C. Wu, J.S. Corneille, C.A. Estrada, J.W. He, D.W. Goodman, Chem. Phys. Lett. 182 (1991) 472.
[30] M.C. Wu, J.S. Corneille, J.W. He, J.W. Estrada, D.W. Goodman, J. Vac. Sci. Technol. A 10 (1992) 1467.
[31] M.C. Wu, C.A. Estrada, J.S. Corneille, D.W. Goodman, J. Chem. Phys. 96 (1992) 3892.
[32] C.M. Truong, M.C. Wu, D.W. Goodman, J. Chem. Phys. 97 (1992) 9447.
[33] C.M. Truong, M.C. Wu, D.W. Goodman, J. Am. Chem. Soc. 115 (1993) 3647.
[34] M.C. Wu, C.M. Truong, D.W. Goodman, J. Phys. Chem. 97 (1993) 4182.
[35] M.C. Wu, C.M. Truong, D.W. Goodman, J. Phys. Chem. 97 (1993) 9425.
[36] J.S. Corneille, J.W. He, D.W. Goodman, Surf. Sci. 338 (1995) 211.
[37] D.R. Rainer, D.W. Goodman, J. Mol. Catal. A: Chem. 131 (1998) 259.
[38] X.P. Xu, S.M. Vesecky, D.W. Goodman, Science 258 (1992) 788.
[39] X.P. Xu, D.W. Goodman, J. Phys. Chem. 97 (1993) 683.
[40] P.J. Berlowitz, D.W. Goodman, Langmuir 4 (1988) 1091.
[41] K. Coulter, X.P. Xu, D.W. Goodman, J. Phys. Chem. 98 (1994) 1245.
[42] D.R. Rainer, C. Xu, P.M. Holmblad, D.W. Goodman, J. Vac. Sci. Technol. A 15 (1997) 1653.
[43] D.R. Rainer, M. Koranne, S.M. Vesecky, D.W. Goodman, J. Phys. Chem. B 101 (1997) 10769.
[44] D.R. Rainer, S.M. Vesecky, M. Koranne, W.S. Oh, D.W. Goodman, J. Catal. 167 (1997) 234.
[45] C. Xu, X.F. Lai, D.W. Goodman, Faraday Discuss. (1996) 247.
[46] C. Xu, W.S. Oh, G. Liu, D.Y. Kim, D.W. Goodman, J. Vac. Sci. Technol. A 15 (1997) 1261.
[47] D. Meier, G.A. Rizzi, G. Granozi, X. Lai, D.W. Goodman, Langmuir 18 (2002) 698.
[48] T.V. Choudhary, S. Chinta, C.C. Chusuei, A.K. Datye, J.P. Fackler, D.W. Goodman, J. Catal. 207 (2002) 247.
[49] M. Valden, X. Lai, D.W. Goodman, Science 281 (1998) 1647.
[50] C.C. Chusuei, X. Lai, K. Luo, D.W. Goodman, Top. Catal. 14 (2001) 71.
[51] X. Lai, T.P. St Clair, M. Valden, D.W. Goodman, Prog. Surf. Sci. 59 (1998) 25.
[52] X.F. Lai, D.W. Goodman, J. Mol. Catal. A: Chem. 162 (2000) 33.
[53] D.W. Goodman, Ann. Rev. Phys. Chem. 37 (1986) 425.
[54] M.A. Vannice, J. Catal. 44 (1976) 152.
[55] M.A. Vannice, Catal. Rev. Sci. Eng. 14 (1976) 153.
[56] X.P. Xu, J. Szanyi, Q. Xu, D.W. Goodman, Catal. Today 21 (1994) 57.
[57] S.H. Oh, C.C. Eickel, J. Catal. 128 (1991) 526.
[58] S.M. Vesecky, P.J. Chen, X.P. Xu, D.W. Goodman, J. Vac. Sci. Technol. A 13 (1995) 1539.
[59] S.M. Vesecky, D.R. Rainer, D.W. Goodman, J. Vac. Sci. Technol. A 14 (1996) 1457.
[60] B.K. Cho, J. Catal. 131 (1991) 74.
[61] J.L. Carter, J.A. Cusumano, J.H. Sinfelt, J. Phys. Chem. 70 (1966) 2257.
[62] M.C. Desjonqueres, F. Cyrot-Lackmann, J. Chem. Phys. 64 (1976) 3707.
[63] M. Kiskinova, D.W. Goodman, Surf. Sci. 108 (1981) 64.
[64] D.W. Goodman, Catal. Today 12 (1992) 189.
[65] G.A. Martin, J. Catal. 60 (1979) 452.

[66] M. Haruta, M. Date, Appl. Catal. A 222 (2001) 427.
[67] A. Sanchez, S. Abbet, U. Heiz, W.D. Schneider, H. Hakkinen, R.N. Barnett, U. Landman, J. Phys. Chem. A 103 (1999) 9573.
[68] T. Hayashi, M. Haruta, Shokubai (Catalysts Catal.) 37 (1995) 72.
[69] J.H. Fendler, Chem. Mater. 8 (1996) 1616.
[70] A. Henglein, Chem. Rev. 89 (1989) 1861.
[71] M.B. Mohamed, C. Burda, M.A. El Sayed, Nano Lett. 1 (2001) 589.
[72] M. Valden, S. Pak, X. Lai, D.W. Goodman, Catal. Lett. 56 (1998) 7.
[73] J. Szanyi, W.K. Kuhn, D.W. Goodman, J. Vac. Sci. Technol. A 11 (1993) 1969.
[74] C.M. Truong, J.A. Rodriguez, D.W. Goodman, Surf. Sci. 271 (1992) L385.
[75] V.A. Bondzie, S.C. Parker, C.T. Campbell, J. Vac. Sci. Technol. A 17 (1999) 1717.
[76] Z.X. Yang, R.Q. Wu, D.W. Goodman, Phys. Rev. B 61 (2000) 14066.
[77] E. Habenschaden, J. Kuppers, Surf. Sci. 138 (1984) L147.
[78] X.F. Lai, T.P. St Clair, D.W. Goodman, Faraday Discuss. (1999) 279.
[79] A. Kolmakov, D.W. Goodman, Catal. Lett. 70 (2000) 93.
[80] A. Kolmakov, D.W. Goodman, Rev. Sci. Instru., in press.